

Pulsed Nd:YAG Laser Dissimilar Welding of Grade 2 Titanium Alloy to 3105-O Aluminum Alloy using AlSi5 Filler Metal

A. A. Shehab¹, Adel K. Mahmoud², S. K. Sadrnezhaad³,
M. J. Torkamany⁴, S. A. Jawad⁵

¹Institute of Laser for Postgraduate Studies, University of Baghdad, Baghdad, Iraq

^{2,5}Department of Mechanical Engineering, College of Eng. Diyala University, Diyala, Iraq

³Department of Materials Science and Engineering, Sharif University of Technology, Tehran, Iran

⁴Iranian National Center for Laser Science and Technology (INLC), P.O. Box 14665-576, Tehran, Iran

Abstract: A special form of laser spot welding is introduced to overlap dissimilar welding of titanium (G2) to 3105-O aluminum alloy. A welding tactile seam tracking design using following pulses that result to a circular seam leads to spot like shape laser welding. This technique was conducted to joint overlapped grad 2 Titanium alloy (Ti G2) to 3105-O Al alloy, with 1, and 0.5 mm thicknesses respectively by using of AlSi5 filler metal with different (0.1, 0.16, 0.22) mm thicknesses. Different types of IMP were formed in the Ti-Al mixing zone. Weld zones in the side of Ti near Ti-Al interface are mainly formed from Ti_3Al and $TiAl$. Microcracks are easily propagating through Ti_3Al , forming longitudinal cracks. The AlSi5 filler metal has a positive effect on the weld Microstructure and thus joint strength, where Si has reduced the IMP ($TiAl_3$) harmful effect via replacing Al atoms substitutionally in $TiAl_3$.

Keywords: Laser Dissimilar Welding; Filler Metal; Microstructure and Mechanical Properties; Aluminum, Titanium Alloys.

Introduction

The titanium and aluminum are light in weight; maintain good strengths to weight ratio besides, superior conductivity and corrosion resistance [1]. These properties candidate aluminum serious 3xxx to be welded to grade 2 titanium pipe as a blade cooling fin in aero plane cabins [2]. The combination of titanium and aluminum, using different welding techniques was the goal of many authors. W. H. Sohn, et al. [3] reported that the formation of several intermetallic phases IMP, such as $Al_5Si_2Ti_7$, $Al_{12}Si_3Ti_5$, due to the diffusion of Si through Ti layer, proceeded bonding at interface between Ti and the AlSi10Mg1 filler metal, where the bond strength at Al-Ti joint, has increased with increasing bonding time up to 25 min at 620 °C and then decreased due to formation of cavities in Al near Al-IMC interfaces. Z. Zhu, et al. [2], has observed an increase in the hardness of the interface and the around regions with some diffusion layers of both Ti-6Al-4V and A6061 alloys across the interface, that increased with the diffusion time of ultrasonic welding. C. Yu-hua, et al [4], found that with the increase of welding speed or the decrease of tool rotation rate during FSW, the amount of stirred Ti alloy particles into the stir zone via tool pin force, decreases, and cracks are presented on interface and thus the failure loads of the joints decreases.

The joining of Ti and Al by conventional fusion welding process a real challenge due to the difference in thermo physical properties and lattice structure. In addition there is a limited solubility of Al in Ti, whereas a solid solution up to about 12 at% Al can be obtained towards Ti-rich alloy. On the aluminium rich side, the maximum solubility of Ti in Al does not exceed 2 at. %. This limited solubility of titanium on the aluminum rich side leads to an early formation of the IMP $TiAl_3$, when the titanium content, exceeds approx. 2at.% [5]. Also the system has very high value of negative enthalpy of mixing [6], thus as Al melts first by conventional fusion welding, Ti dissolves in it and forms mostly Al_3Ti , $TiAl$, Ti_3Al .

Recently laser has been used to join these material, it provides many advantages over conventional welding such as high quality, high precision, high performance, high speed, good flexibility and low distortion [7]. Maunder, et al. [6] concluded that it was impossible to obtain Al content below 20 at% in the Al-Ti mixing zone, and crack free weld by any combination of process parameters during CO₂ laser welding of Ti-6Al-4V and AlMg0.9Si. They observed that the sandwiching of a Nb plate between Ti and Al sheets kept of 11 at.% Al content in the FZ and formed TiNb solid solution with crack free joint. These conclusions have pushed to the choice of filler metals addition to the weld joint of Ti-Al, in order to improve the weld metallurgy and control the IMP formations.

Y.Chen, et al.[8,9] investigated the effect of heat input on microstructure and mechanical property of Al-Ti interface during laser welding-brazing with AlSi12 filler. They founded that low heat input leads to form dissolution mod of Ti in the filler metal (thin layer of IMP is formed), and fracture at the fusion zone with high value of tensile strength, with increasing heat input (melting mod of Ti in filler) the IMP thickness increases and fracture occurred at the interface or at the fusion zone due to porosity formation. Liqun Li, et al. [10] investigated the mechanism of joining Al/Ti during CO₂ laser welding-brazing butt joint, with AlSi12 filler. They found that the microstructures of brazing zone are composed of α -Ti nano size, Ti₇Al₅Si₁₂ and TiAl₃, while α -Al and ternary structure with α -Al, Si and Mg₂Si were observed in the welding zone. They concluded that the formation of Ti₇Al₅Si₁₂ weakened the dissolution of Ti, and thus suppressed the growth of TiAl₃. Liu De-jian, et al. [11] investigated the Si diffusion behavior during CO₂, CW laser welding-brazing of Al to Ti alloys, using AlSi12 filler wire they found that the Si diffusion behavior is more affected by Ti content than that of the temperature, where in the case of Ti melting mode(welding), Si diffuses to liquid Ti, besides gets together at the interface. In the present work the microstructure and mechanical properties were investigated during pulsed Nd:YAG laser welding of Ti to Al using AlSi5 filler metal.

Experimental Work

ASTM titanium grade two TiG2 and 3105-O aluminum alloy were chosen for the present work with 1, 0.5 mm thicknesses respectively. The metal sheets were cut into 40 x 5 mm pieces. AlSi12 filler metal with three different thicknesses 0.1, 0.16 and 0.22 mm was sandwiched between Ti and Al during welding. The chemical composition and mechanical properties for both Al and TiG2 alloys are listed in Table1 [12]. The surfaces of the sheets were cleaned and degreased by acetone and polished, then Al sheets cleaned with 6-10%NaOH alkaline for 5minutes and rinsed with tap water followed by 30% HNO₃ + 3% H₂SO₄ acid solution for 3 minutes. Ti sheets were cleaned with 20% HNO₃ + 5% HF acid solution for 5minutes then wiped and rinsed with ethanol and tap water. The cleaning processes were done just 10 minutes before welding

The welding experiments of the present work, were done by using pulsed Nd:YAG laser Model IQL-10, with average power of 400 W and standard square shape pulse, as the welding laser source. The ranges for the laser parameters were: 1–1000 Hz for pulse frequency, 0.2–20 ms for pulse duration, and 0–40J for pulse energy. A 5000 W-LpOphir power meter and LA300 W-LP Joule meter were used to measure average power and pulse energy respectively. The focal length of focusing optical system was 75 mm providing of about 250 μ m laser spot size. A movable XYZ table was used to move the clamping device with an accurate speed under laser head with 0.05 mm positioning precision. A coaxial nozzle with the laser beam provides argon shielding gas with purity of 99.999%, on top of the weld line. The argon gas flow rate was fixed to 20 L/m, due to sensitivity of both Ti and Al to atmospheric conditions. The minimum focused laser diameter was 0.25 mm, the laser spot focused diameter at the surface of the metal sheet to be welded was 0.4 mm.

The tensile testes were done by using SANTA, model STM-20, Universal Testing Machine, 5 mm/min cross head speed was used. An average of at least two tested samples was calculated. After welding the samples were wire cut near the welding zone. A grinding and polishing process by using abrasive silicon carbide papers of range (600,800 and 1200,2000,3000) grain/cm², were used to grind and polishing the samples Additional polishing using solution of water and alumina particles of 3 different grain sizes was used, in each stage of polishing, a certain grain size was used, with the polishing clothe.

The Microstructure of weld zone was etched using fresh prepared Kroll reagent for 30s. Dissimilar weld zone appearance, geometry, microstructure and fracture zone of the joints, were investigated by means of optical microscope and optical microscope, scanning electron microscopy (SEM), TESCAN MIRA 3, Austria, equipped with energy dispersive X-ray spectrometry (EDS). For exact phase determination at the fractured surface, x-ray diffraction (XRD), PAN, Model X'Pert, equipped with PIXcel detector and X'Pert high score plus (V.3) software were used. The Vickers micro hardness values were measured by using of BUEHLER model MMT1, USA micro hardness tester, with a 25 g loading force for 25 second. An average of three measured readings was calculated for selected locations (BM, HAZ, and FZ), for each side of the dissimilar joint.

Table 1: Chemical Composition by Weight for the Used Material [17]

Material type	Percentage%									
	Element	C	Mn	Si	Zn	O	Mg	Cu	Fe	Al%
Al3105-O	-	0.51	-	0.06	-	0.5	009	061	Bal.	-
ASTM Ti G2	0.08	-	-	-	0.2	0	0	0.08	-	Bal.
AlSi5(4043)	-	0.004	4.5	0.016	-	<0.2	0.11	0.16	Bal.	-

Table 2: Mechanical Properties of the Base Material [17]

Property	Al3105-O	ASTM Ti G2
UTS (MPa)	122	344
YTS (MPa)	55	275
Shear Stress (MPa)	82	-
Hardness (HV)	45	125
Elongation (%)	24	28

Results and Discussion

Based on the pretest experiments, it was impossible to laser spot welding of Ti to Al, with acceptable joint strength levels, by conventional way, i.e. using single or several pulses at the same position, whatever the combinations between pulse duration and pulse peak power are, and this could be related to limited solubility of each metal in the other and the gap between thermophysical properties of Ti and Al, where the samples that were welded, have fractured, while trying to get them from the clamping device. Thus a circular seam welding path (see Figure 1) that leads to spot weld was a unique solution for laser spot welding of Ti to Al comparing with conventional laser spot welding method. In pulsed laser welding the energy ejected to an area comes not only from a single pulse but also from pulses overlapping. The overlapping factor PER can be calculated from equation 1[13]:

$$PER = 1 - \frac{v \cdot PRT}{2\omega + v \cdot \tau} \quad (1)$$

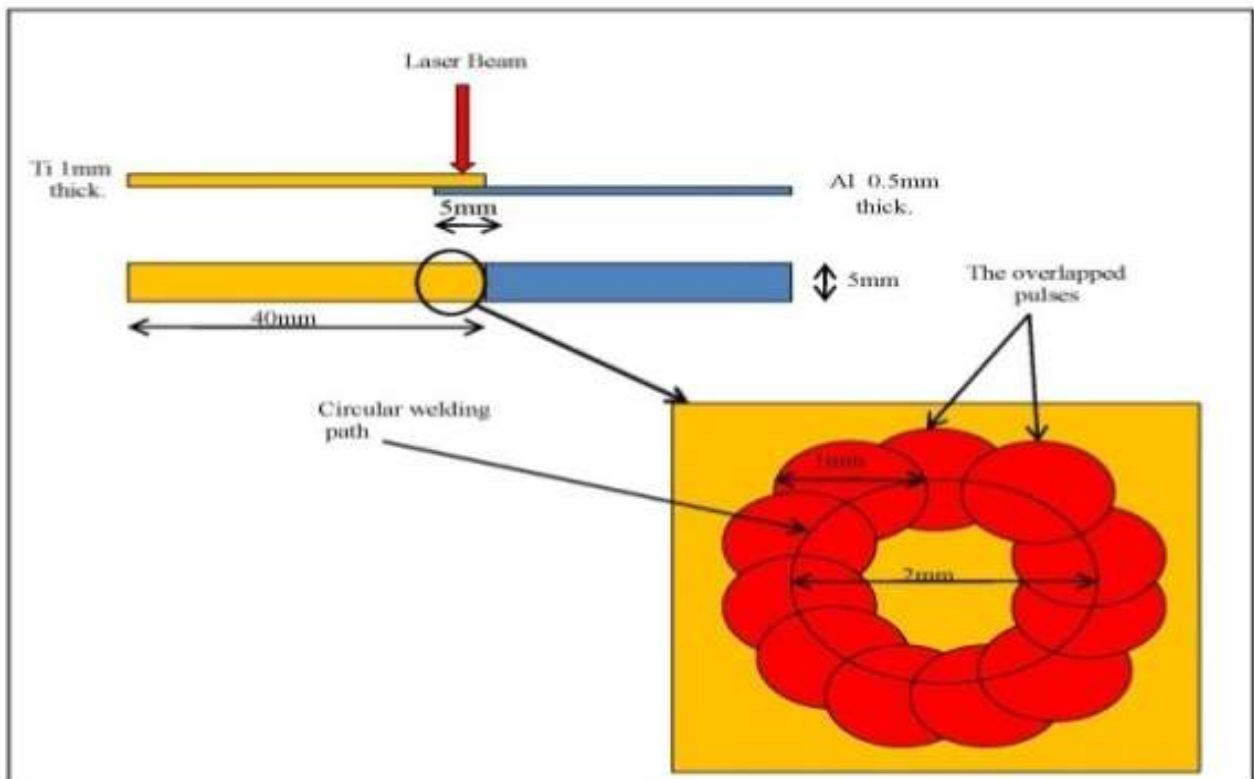


Figure 1: Joint design and welding Path

Via putting the values of pulse repetition rate(PRT)=1/pulse frequency(20Hz), pulse duration (τ) = 6 ms, focused spot at the target surface (w) = 0.4 mm, in eq. 1, a PER of 76 % can be obtained. The average energy input per unit area (E_a), for a given laser spot size (ω) can be calculated using eq.2 [13]:

$$E_a = \frac{E_{pulse} \times \text{pulse frequency}}{v \cdot \omega} \quad (2)$$

to get value of 137.5 J/mm². Based on the pretest experiments, the laser welding parameters are fixed and presented in Table 2, while using different thicknesses of AlSi5 filler metal.

Table 3: Laser welding parameters

Sample No.	AlSi5 filler thick.(mm)	Pulse energy (J)	Pulse duration (ms)	Welding speed (mm/sec)	Peak power (kW)	Pulse frequency (HZ)	Argon gas flow rate(L/min)	Average Energy input perunitarea(J/mm ²)
4	0.1	11	6	4	1.83	20	20	137.5
5	0.16	11	6	4	1.83	20	20	137.5
6	0.22	11	6	4	1.83	20	20	137.5

Weld Appearance. Figure 2 shows the top and bottom surface appearance of Ti-Al laser welded joints for samples 4, 5 and 6 respectively. It can be seen from this figure that increase the thickness of the filler metal reduces the weld bead dimensions for the same welding conditions where thicker filler material consume more energy during its melting and also conducts more heat to the surrounding materials, this lost energy is taken from the ejected laser and thus leads to reduce the weld bead dimensions.

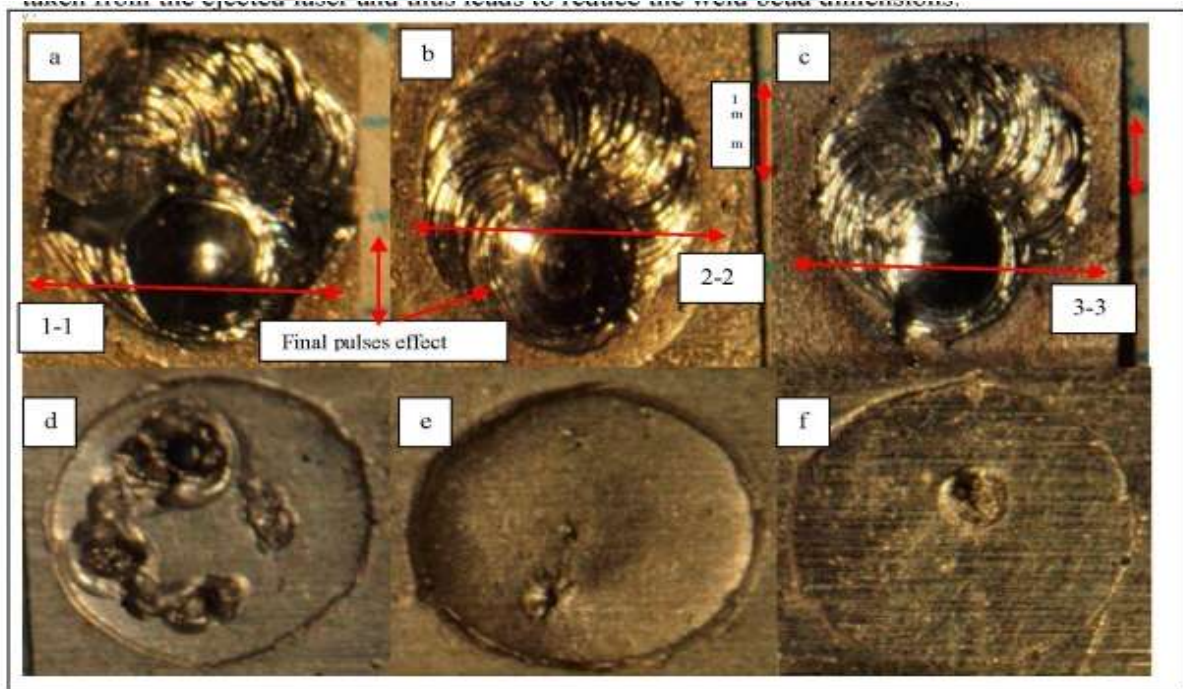


Figure. 2: The top and bottom surface appearance of Ti/Al laser welded joints for: a,d. sample 4; b,e. sample 5; c,f. sample 6 respectively

Figure 3 shows the weld cross sections of Figure 2. It can be seen from this figure that porosities are generated in the weld cross sections especially for the final pulses effect, at end point of the circular welding path, where about three pulses are ejected at the same place, during the time interval between machine movement stop and laser power supply stop, thus big circular dips are formed. Due to the effect of gap between welded sheets, porosity is seen in this figure where this type of porosity is common in lap joint design [14]. The low viscosity of molten aluminum, limits its expansion before solidification, besides its high coefficient of thermal expansion leads to strong contraction during the solidification, thus large change in the volume of the metal upon melting and solidification is occurred which may lead to weld bead holes (large porosity) near the final pulses effect[15,16]. Also the vaporized low melting Mg that contained in the filler AlSi5 metal is one of the reasons that lead to porosity formation.

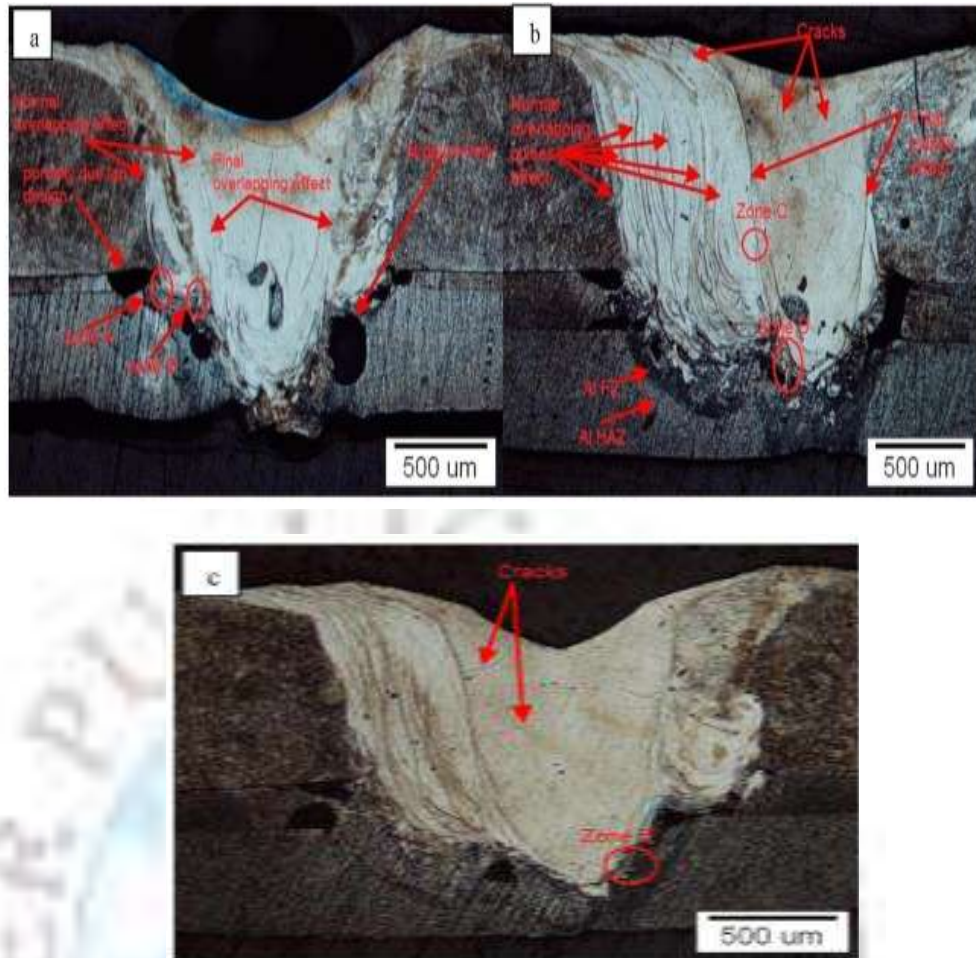


Figure. 3: Weld cross sections of Fig.2: a.section1-1; b.section2-2; c.section3-3.

Cracks are observed at the upper surfaces and weld bead of Ti sheet for samples 5 and 6 in Figure 3.b,c due to high cooling rate (quenching effect) that leads to acicular α - martensite and some IMP formation and this will be discussed in section 3.2.

Weld Microstructure. Figure 4 shows zone (c) in Figure 3.b. Two zones are observed from this figure, the zone of normal overlapping pulses (76% overlap), where an acicular-martensite microstructure formation is clearly observed from this figure as a result of high cooling rate where the results of microhardness indicate a value up to 500 HV, that agrees with the literature [17] as a result, micro cracks are formed in this zone which are transgranular in nature [6]. The other zone is the zone of final pulses effect where the high heat

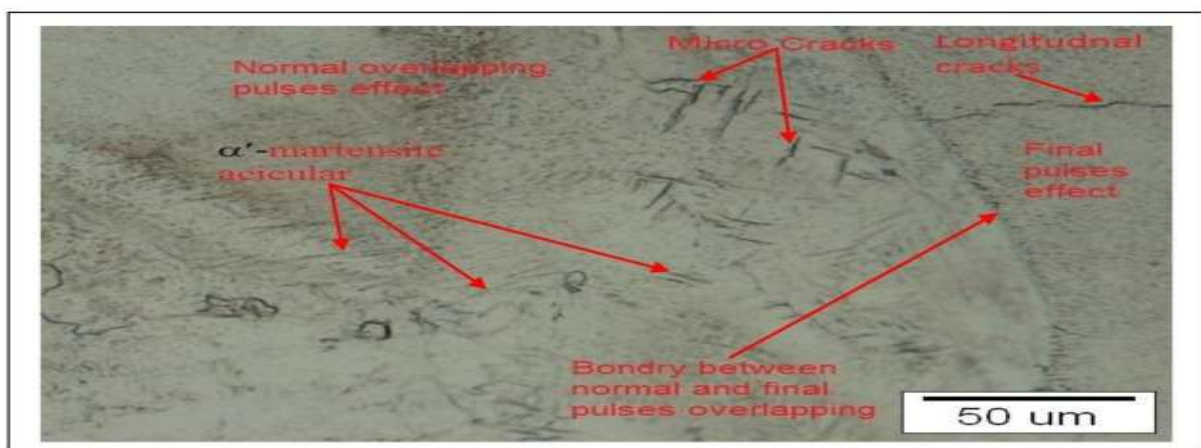


Figure. 4 Zone (c) in Fig. 3.b

input (more time of Ti-Al interaction), due to ejection of about 3 pulses at the same location, leads to IMP (Ti₃Al) formation as indicated by EDS analysis and thus high microhardness values of more than 500 HV was obtained in this zone where the microcracks are easily propagated through IMP, forming longitudinal microcracks. Figure 5 shows the optical and SEM images of zones that presented in Figure 3. The EDS patterns of point scan analysis of Figure 5 are presented in Figure 6, and the weight and atomic analysis results are presented in Table 3. It can be seen from both Figure 5.a, and Table 3 that Si atoms diffuse in

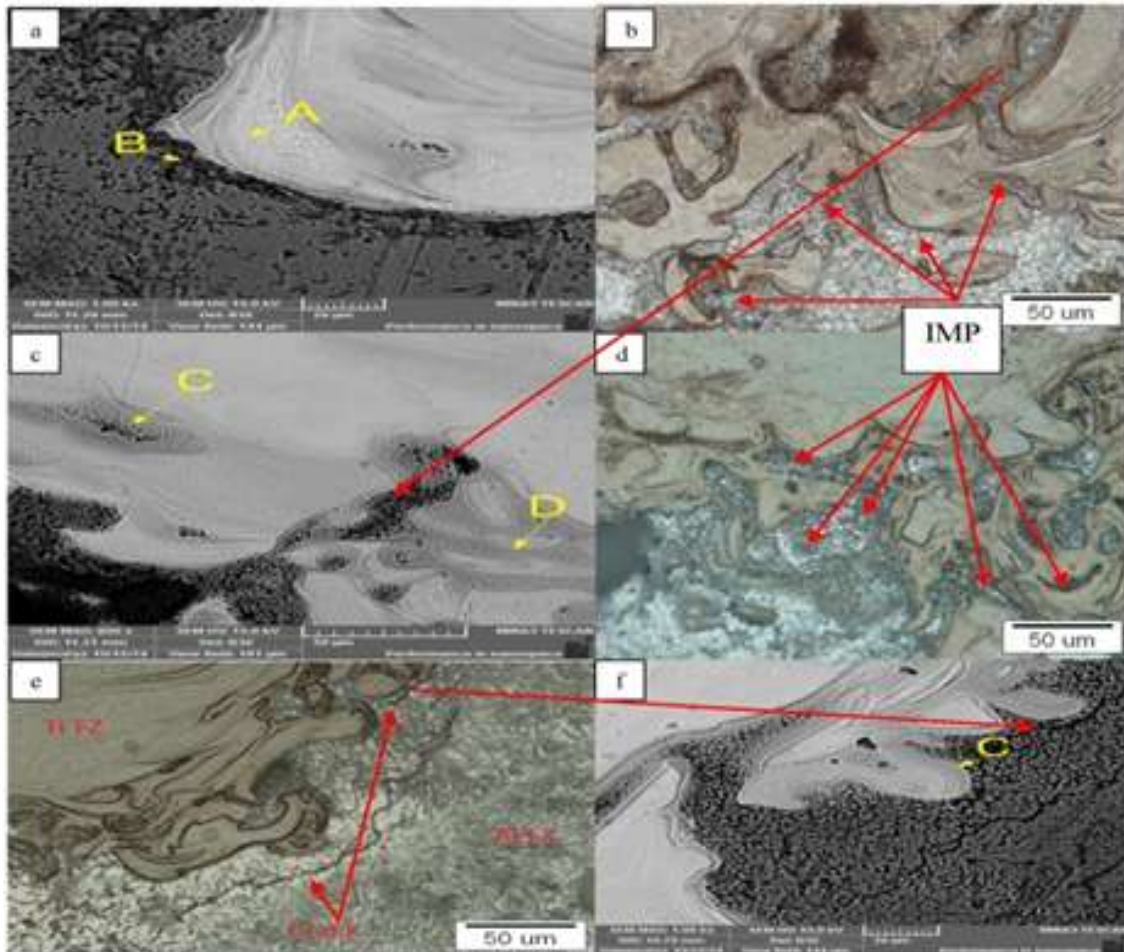


Figure 5: Optical and SEM images of zones Fig. 3: a. SEM image of zone A; b,c. optical and SEM images of zone B respectively; d. optical image of zone D; e,f. optical and SEM images of zone E respectively.

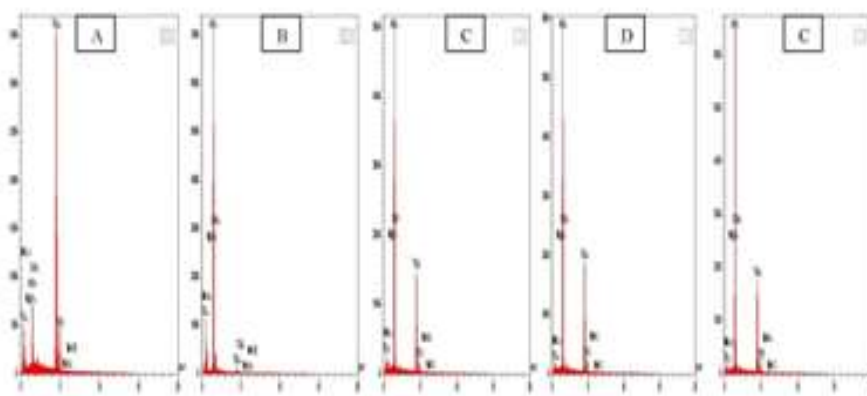


Figure 6: EDS patterns of point scan of the yellow colored points of Fig.5 respectively

molten titanium at the Ti-Al interface thus restricts the mixing of Ti with Al, via replacing Al atoms in IMP Ti₃Al₃ lattice structures, due to the adjacent atomic radii between Si and Al and thus reduce the formation TiAl₃ and its harmful effect at

the Ti-Al interface. Different colors brightness in the optical images Figure 5.b,d are referred to different IMP formation. It is seen from

Tables 4: Weight and atomic analysis of Al ,Ti and Si elements of Fig. 5.a,c and f respectively

Fig.5	Point	Element Ti		Element Al		Element Si		TixAly phase	comments
		Wt%	At%	Wt%	At%	Wt%	At%		
a	a	97	94.8	2.7	4.7	0.23	0.39	Ti-al solid solution(α)	(Ti-Al) solid solution
	b	9.5	5.6	81.9	85.9	7.6	0.6	TiAl ₃	IMP Ti(Al,Si) ₃ , Si is replacing Al in TiAl
c	c	65	51.6	34	46.8	0.5	0.69	TiAl	IMP
	d	68	55	30.7	43.9	0.33	0.45	TiAl	IMP
f	c	64.4	51	34	47	0.61	0.6	TiAl	IMP

Table 4 that weld zones in the side of Ti near the Ti-Al interface are mainly formed from Ti₃Al and TiAl that have higher strength values comparing with TiAl₂ and TiAl₃, because the strength of TixAly increases as Ti content increases [18]. The solidification cracks that were formed in the zone of resolidified Al, near Ti-Al interface Figure 5.e,f, are due to localized strain as a result of strength gradient between Ti FZ near the Ti-Al and the surrounded Al resolidified zones, where some IMP that were formed in between these regions do not have ductility to withstand this strain[19]. Also the residual stress induced by the difference between thermal expansion coefficient of Ti and Al have a negative effect in preventing crack initiation and propagation[20]. These cracks are intergranular in nature perpendicular to the solidification direction and associated with high cooling rate(i.e. samples 5 and 6) [6].

Mechanical Properties

Shear Strength of the Joint. Figure 7, shows shear force vs. extension in addition to weld seam shape, at bottom interface surface of Ti sheet for samples 4, 5, and 6. A higher shear force (256N) value, for the joint of sample 4 is observed when comparing with samples 5 (246N) and 6 (218N) and this could be related: first to wider more uniform melted area Ti-Al interface in lap design where higher heat (lower thickness of AlSi5 filler metal) is responsible for this melted area, and second to transgranular (micro and longitudinal) cracks that formed in Ti FZ near Ti-Al interface due to embrittlement as a result of cooling rate for samples 5 and 6(see Figure 3.b,c and Figure 4) where the joint strength in lap design is mainly depending on area at interface in addition to weld strength [1,21]. The optical and SEM images of the fractured sample under shear load for samples 4, 5, and 6 are presented in Figure 8. It can be seen from Figure 8.a that sample 4 has fractured from zone occurred at Al resolidified zone not Ti-Al, as a result of: low strength of this zone; IMP and porosity formation where both types of fracture (brittle and ductile) are observed (see Figure 8 d, g.). The XRD device could not be used for sample 4 due to small fractured surface area that can be subjected to the test. Samples 5 and 6 have fractured from Al-Ti interface near Al resolidified zone, and this seems to be due to IMP formation and the harmful effects of solidification cracking that formed near IMP zones ,see Figure 8.b,c.

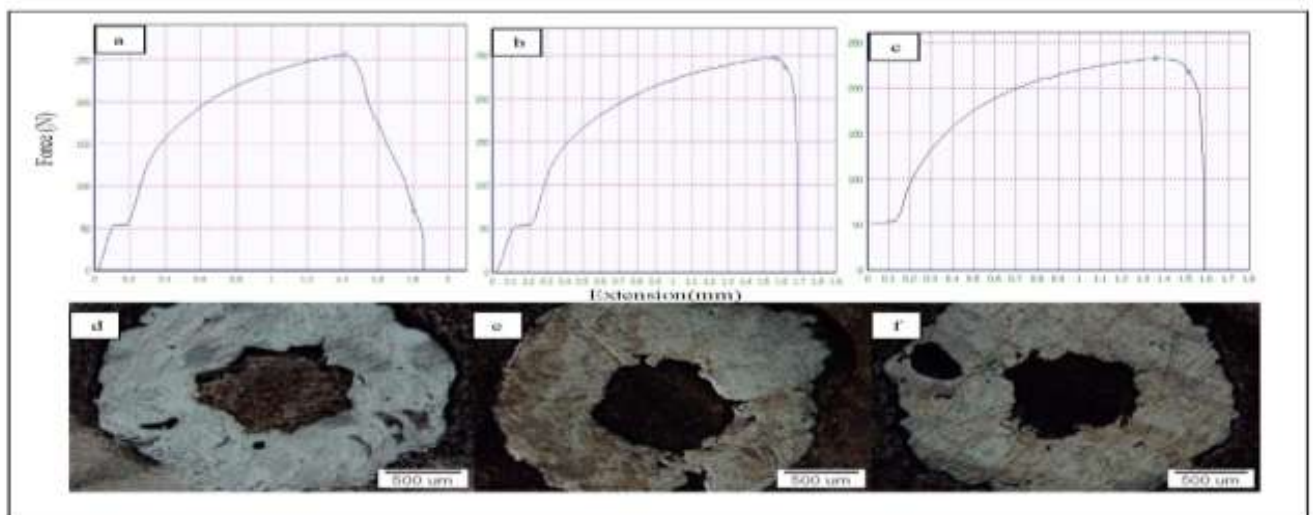


Figure 7 : Shear force vs. extension in addition to weld seam shape, at bottom interface surface of Ti sheet for samples 4,5, and 6 respectively : a,d. sample 4; b,e. sample 5; and c,f. sample 6

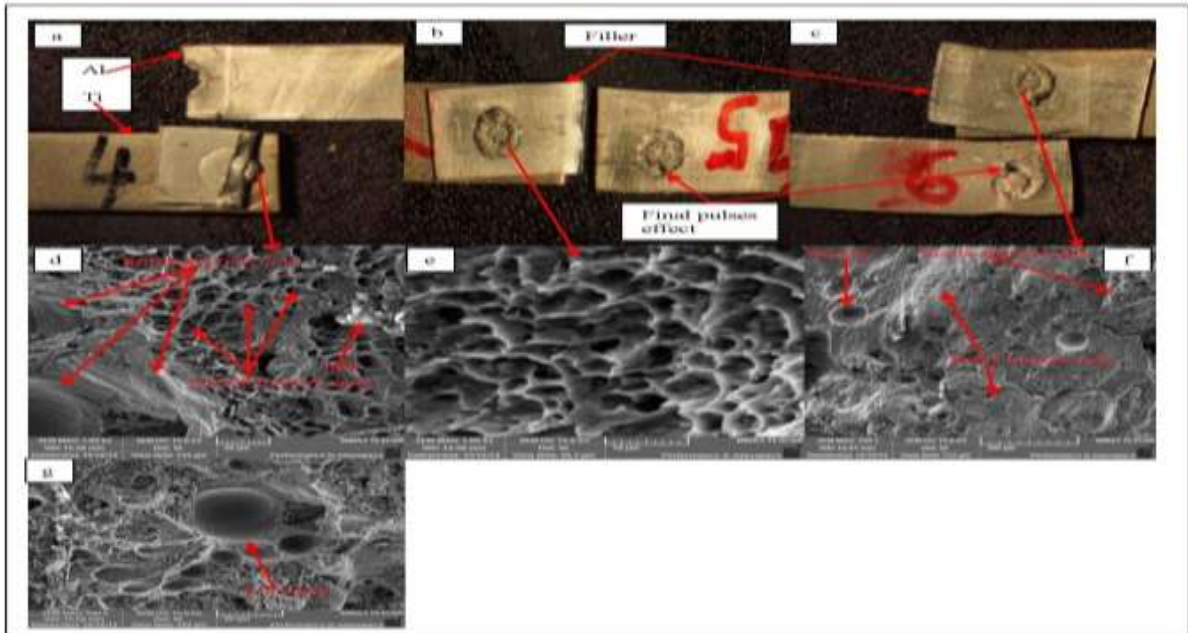


Figure 8: Optical, and SEM images of fractured of samples 4,5 and 6: a,d,g, for sample 4; b,e, for sample 5; and c,f, for sample 6

A zone of ductile fracture can be observed for sample 5 compared with sample 6 that have both brittle and ductile fractures see Figure 8.e,f and this could be related to lower cooling rate (lower thickness of filler metal than 6) and thus more time for Si diffusion in molten Ti to form triple alloy AlSiTi, see the green peak in Figure 9.a., which is not observed in case of sample 6, see Figure 9.b. Therefore the time that was available for sample 4 (lower thickness filler compare with samples 5 and 6, for Si to diffuse in TiAl3 (see Table 3 point. b), may be one of the reasons that improved Ti-Al interface and prevents the occurring of the fracture at that zone. The multi peaks of TiAl3 IMP that observed at the fractured surface of samples 6 in XRD patterns Figure 9.b, gave indication that TiAl3 is focused in a certain area that leads to the brittle fracture. It is important to note that when fixing .

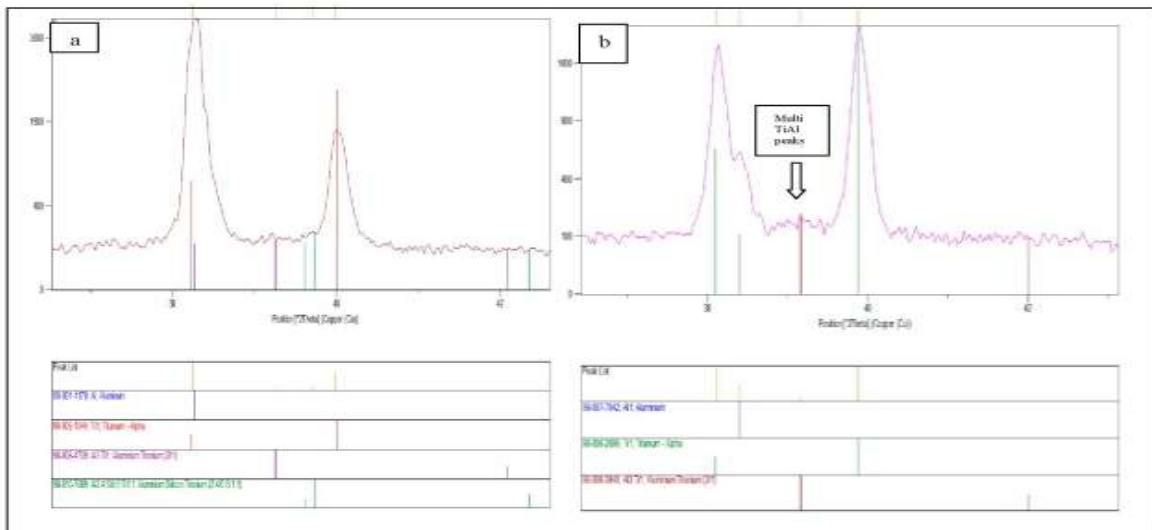


Figure 10 Shear stress values of: 1.sample 4; 2.shear stress of Al bas metal; 3. tensile stress of Al bas metal.

Microhardness of the Joint. The microhardness measurements locations (BM, HAZ, and FZ) for each side of the dissimilar joint are presented in Figure 11 for samples 4, 5 and 6 respectively, where the values of microhardness are listed in Table 4. It can be seen from this table for the Ti side that dramatic increase Ti FZ microhardness values compared with the Ti BM (125HV). The formation of acicular α' -martensite as a consequence of laser welding thermal cycles (quenching effect), seems to be responsible for this increase (see Figure 4) [17]. Also the possibility for IMP formation in Ti upper side FZ specially for the effect of final pulses where a strong interaction that occurs between Ti and Al is responsible for hardness values increase. The hardening effect observed in the Ti-Al dissimilar weld interface

is related to the IMP formation where a higher microhardness values compared with the other zones are observed at the Ti-Al weld interface (see Figure 11 and Table 4). For the Alside there is a decrease in microhardness values for Al HAZ when comparing with the Al BM (46HV), where the material is subjected to grain growth and thus coarsening. The resulting hardness increase in Al FZ compared with the corresponding Al BM due to grain refining as a result of high cooling rate for laser welding processes.

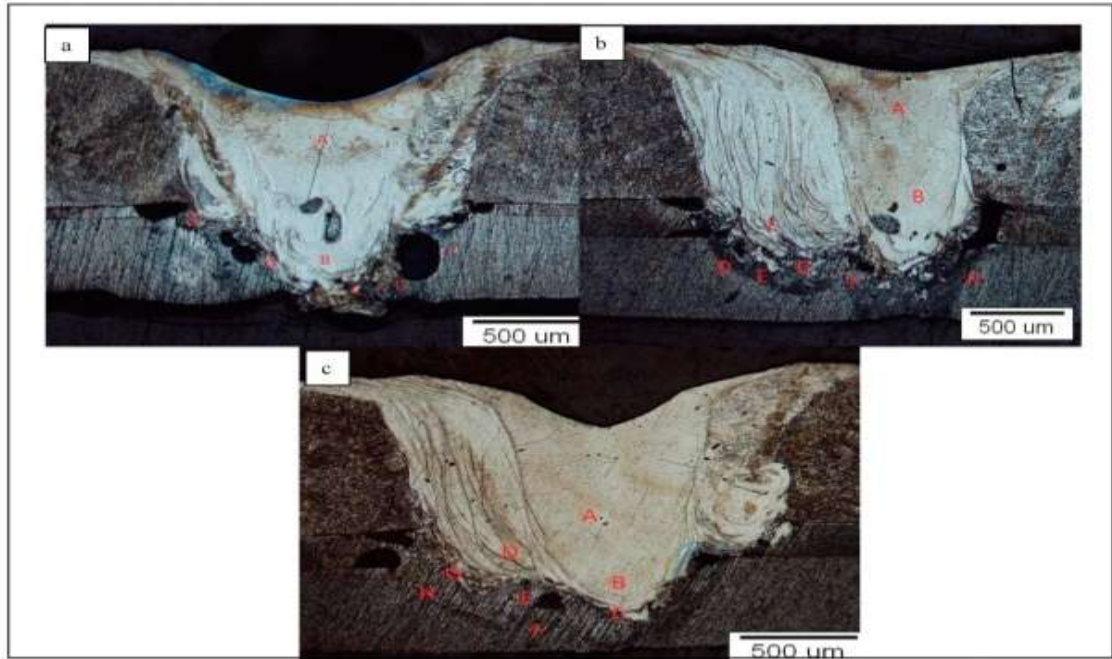


Figure 11: Microhardness measurements for different locations of Ti/Al laser welding joint, for samples No.; a.4; b.5 and c.6 respectively

Table 4: Values of microhardness for the points that located in Figure 11

Sample No.	Point	Microhardness (HV)	comments
4	A	473	TiFz
	B	464	TiFz
	C	503	IMP
	G	51.3	AlFz
	F	43	AlHFz
	D	599	IMP
	E	420	IMP
5	A	473	TiFz
	B	397	TiFz
	C	503	TiFz
	D	24	AlHFz
	E	54	AlFz
	F	49	AlFz
	G	599	IMP
	H	32	AlHFz
6	A	413	TiFz
	B	484	TiFz
	C	429	IMP
	D	503	TiFz
	E	54.4	AlFz
	F	32	AlHFz
	H	24.5	AlHFz
	G	626	IMP

Conclusion

A pulsed Nd:YAG laser welding of dissimilar metals, Titanium grade two 1mm thickness to 3105-O Al alloy, 0.5 mm thickness, by using of AlSi5 filler metals with different (0.1, 0.16, 0.22) mm, thickness has been investigated experimentally regarding to joint's microstructure and strength. Based on the experimental results and discussion the following points are concluded:

1. The window of laser welding parameters of Ti to Al was narrow and selected carefully where pulse energy 11 J, pulse duration 6ms, pulse frequency 20Hz, argon gas flow rate 20 l/m and welding speed 4mm/s
2. A tactile seam tracking pulses with circular path that leads to spot laser welding was a unique method for joining Ti to Al with the advantage of increasing the weld path over very limited available area.
3. Different types of IMP were formed in the Ti-Al mixing zone. Weld zones in the side of Ti near the Ti-Al interface are mainly formed from Ti₃Al and TiAl. Micro cracks are easily propagating through Ti₃Al, forming longitudinal cracks.
4. The AlSi5 filler metal has positive effect on the weld Microstructure, and thus joint strength, where Si has reduced the IMP (TiAl₃) harmful effect via replacing Al atoms substitutionally in TiAl₃.

Acknowledgment

The authors would like to thank Institute of Laser for Postgraduate Studies, University of Baghdad, Sharif University of Technology and Iranian National Center for Laser Science and Technology for their assistance in doing this work.

References

- [1]. F. Möller et al., Combined Laser Beam Welding and Brazing Process for Aluminium Titanium Hybrid Structures, *Physics Procedia*, 2011, 12:215–223.
- [2]. Z. Zhu et al., Ultrasonic Welding of Dissimilar Metals, AA6061 and Ti₆Al₄V, *Int. J Adv Manuf. Technol.*, 2012, 59:569–574.
- [3]. Woong H. Sohn et al., Microstructure and Bonding Mechanism of Al/Ti Bonded Joint Using Al10Si1Mg Filler metal, *Materials Science and Engineering A355* (2003) 231/240.
- [4]. C. Yu-hua et al., Interface Characteristic of Friction Stir Welding Lap Joints of Ti/Al Dissimilar Alloys, *Trans, Nonferrous Met. Soc. China* 22(2012) 299_304.
- [5]. ASM Handbook of Alloy Phase Diagrams, Volume 3. ASM International. 1993.
- [6]. B. M. Ajumdar et al., Formation of a Crack-Free Joint Between Ti Alloy and Al alloy by Using A High-Power CO₂ Laser, *Journal of Materials Science* 1997, 32, 6191–6200.
- [7]. Seiji Katayama, *Handbook of Laser Welding Technologies*, Woodhead Publishing, Limited, 2013.
- [8]. Yanbin Chen et al., Effects of Heat Input on Microstructure and Mechanical Property of Al/Ti joints by Rectangular Spot Laser Welding-Brazing Method, *Int. J Adv Manuf. Technol.*, 2009, 44:265–272.
- [9]. S. H. Chen et al., Interfacial Reaction Mode and Its Influence on Tensile Strength in Laser Joining Al alloy to Ti alloy, *Materials Science and Technology* 2010, Vol. 26, No. 2.
- [10]. S. Chen et al., Joining Mechanism of Ti/Al dissimilar alloys during laser welding-brazing process" *Journal of Alloys and Compounds* 509 (2011) 891–898.
- [11]. C. Shu-hai et al., Si Diffusion Behavior During Laser Welding-Brazing of Al alloy and Ti alloy With Al-12Si Filler Wire, *Trans. Nonferrous. Met. Soc. China*, 20(2010) 64-70.
- [12]. ASM Handbook, Properties and Selection: Nonferrous Alloys and Special-Purpose Materials, Volume 2. ASM International. 1992.
- [13]. Y. Tzeng. Process Characterization of Pulsed Nd:YAG Laser Seam Welding. *Advanced Manufacturing Technology*, 2000; 16:10 – 18.
- [14]. Katayama S. Formation Mechanisms and Preventive Procedures of Laser welding Defects, 2004 LMP Symposium on High Quality and New Trend of Laser Welding, Laser Materials Processing (LMP) Research Committee of Japan Welding Engineering Society (JWES), 2005, January, 8-1–8-15.
- [15]. Elijah Kannatey, et al. *Principles of Laser Materials Processing*, John Wiley & Sons, Inc., USA, 2009.
- [16]. W. Duley, *Laser Welding*, John Wiley & Sons, Inc., New York, 1998.
- [17]. Seiji Katayama, *Handbook of Laser Welding Technologies*, Woodhead Publishing, Limited, 2013.
- [18]. M. Kreimeyer et al., *Laser Processing of Aluminum–Titanium–Tailored Blanks*, *Optics and Lasers in Engineering*, 43, (2005) 1021–1035.
- [19]. G. Tempuset et al., Improving Interfacial Properties of a laser Beam Welded dissimilar joint of aluminium AA6056 and titanium Ti6Al4V for Aeronautical applications, *J Mater Sci.* 2010, 45:6242–6254.
- [20]. Z. Song et al. Interfacial microstructure and mechanical property of Ti6Al4V/A6061 dissimilar joint by direct laser brazing without filler metal and groove, *Materials Science & Engineering, A* 560 (2013) 111–120.
- [21]. Maruzen, *Metals Data Book*, The Japan Institute of Metals, 2004, p. 215.